NUSC Technical Report 6511
18 September 1981

(15) LEVEL II

Image Theory EM Fields Of Horizontal Dipole Antennas In Presence of Conducting Half-Space

Peter R. Bannister
Submarine Electromagnetic Systems Department

Naval Underwater Systems Center
Newport, Rhode Island / New London, Connecticut

Preface

This report was prepared under NUSC Project No. A59007, "ELF Propagation" (U), Principal Investigator, P. R. Bannister (Code 3411); Navy Program Element No. 11401 and Project No. X0100, Naval Electronic Systems Command, Communications Systems Project Office, Dr. D. C. Bailey (Code PME 110), Program Manager, ELF Communications, Dr. B. Kruger (Code PME 110-X1).

The Technical Reviewer for this report was Dr. Rene Dube.

Reviewed and Approved: 18 September 1981

David F. Dence

David F. Dence
Head, Submarine Electromagnetic Systems Department

The author of this report is located at the New London Laboratory, Naval Underwater Systems Center New London, Connecticut 06320.

REPORT DOCUMENTATION PAGE

READ INSTRUCTIONS BEFORE COMPLETING FORM

1. REPORT NUMBER: NUSC TR 6511	2. GOVT ACCESSION NO.
3. RECIPIENT'S CATALOG NUMBER	
4. TITLE (and Subtitle): IMAGE THEORY EM FIELDS OF HORIZONTAL DIPOLE ANTENNAS IN PRESENCE OF CONDUCTING HALF-SPACE	5. TYPE OF REPORT & PERIOD COVERED
6. PERFORMING ORG. REPORT NUMBER	
7. AUTHOR(s): Peter R. Bannister	8. CONTRACT OR GRANT NUMBER(s): Technical Dept.
9. PERFORMING ORGANIZATION NAME AND ADDRESS: Naval Underwater Systems Center, New London Laboratory, New London, CT 06320	10. PROGRAM ELEMENT, PROJECT, TASK AREA & WORK UNIT NUMBERS: A59007, 1EXD100
11. CONTROLLING OFFICE NAME AND ADDRESS	12. REPORT DATE: 18 September 1981
	13. NUMBER OF PAGES: 28
14. MONITORING AGENCY NAME & ADDRESS (if different from Controlling Office)	15. SECURITY CLASS. (of this report): Unclassified
	15a. DECLASSIFICATION / DOWNGRADING SCHEDULE

16. DISTRIBUTION STATEMENT (of this Report)

Approved for public release; distribution unlimited.

17. DISTRIBUTION STATEMENT (of the abstract entered in Block 20, if different from Report)

18. SUPPLEMENTARY NOTES

19. KEY WORDS (Continue on reverse side if necessary and identify by block number)

Horizontal Dipole Antennas
Image Theory
Finitely Conducting Earth

20. ABSTRACT (Continue on reverse side if necessary and identify by block number)

It is the purpose of this report to extend the use of quasi-static range finitely conducting earth-image theory techniques to the nearfield and farfield ranges. Simple engineering expressions for horizontal electric and magnetic dipole antennas have been derived for the air-to-air, subsurface-to-air, air-to-subsurface, and subsurface-to-subsurface propagation cases. These expressions have been compared with previously derived analytical (or numerical integration) results. For the air-to-air propagation case, the image-theory expressions are valid from the quasi-static

(over)

DD FORM 1 JAN 73 1473

405948

20. (Cont'd)

to the farfield ranges, as long as the square of the index of refraction is large and the Sommerfeld numerical distance is small. For the subsurface-to-air, air-to-subsurface, and subsurface-to-subsurface propagation cases, the additional restriction that the measurement distance be greater than three times the burial depth of the source and/or receiver must be met.

TABLE OF CONTENTS

LIST OF ILLUSTRATIONS

LIST OF TABLES

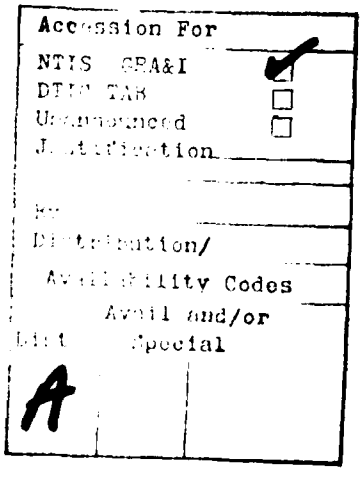

IMAGE-THEORY ELECTROMAGNETIC FIELDS OF HORIZONTAL DIPOLE ANTENNAS IN PRESENCE OF CONDUCTING HALF-SPACE

INTRODUCTION

During the past several years, finitely conducting earth-image theory techniques have proved quite useful in determining the quasi-static fields of antennas located near the earth's surface for both single-layered and multi-layered earths. (For detailed references, see Bannister.[1,2]) The quasi-static range is defined as that range where the measurement distance is much less than a free-space wavelength.

Physically, the essence of the quasi-static range finitely conducting earth-image theory technique is to replace the finitely conducting earth by a perfectly conducting earth located at the (complex) depth d/2, where $d = 2/\gamma_1$ and $\gamma_1 = [i\omega\mu_0(\sigma_1 + i\omega\varepsilon_1)]^{1/2}$ is the propagation constant in the earth. (See figure 1 for the image-theory geometry.) Analytically, this corresponds to replacing the algebraic "reflection coefficient," $(u_1 - \lambda)/(u_1 + \lambda)$, in the exact integral expressions by $\exp(-\lambda d)$, where λ is the variable of integration.[3] For antennas located at or above the earth's surface, the general image-theory approximation is valid throughout the quasi-static range.[1,2]

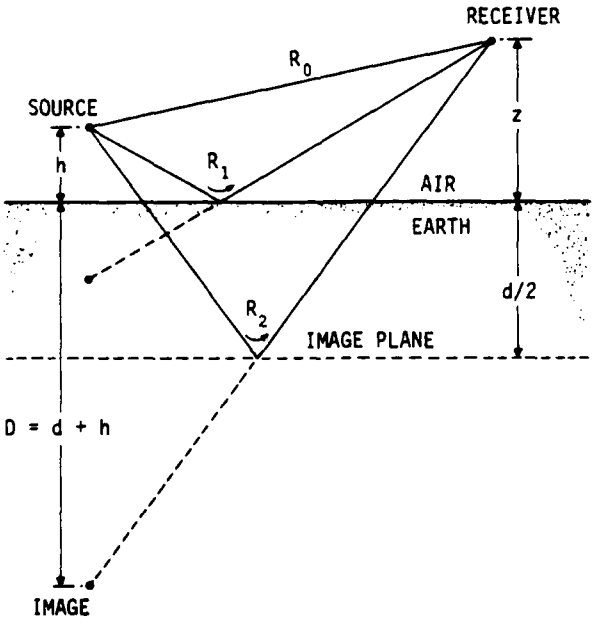

Figure 1. Image-Theory Geometry

The major disadvantage of the finitely conducting earth-image theory technique is that mainly it has been applied only in the quasi-static range. However, because this range includes the critical launching area, one would expect to be able to extend it into the intermediate range where the principal field propagation proceeds as though it were over a perfectly conducting plane.

Recently[2,4] we have shown, for horizontally polarized sources, that finitely conducting earth-image theory techniques are not limited to the quasi-static range alone. That is, by replacing the horizontally polarized algebraic "reflection coefficient," $(u_1 - u_0)/(u_1 + u_0)$, by $\exp(-u_0 d)$, we demonstrated that finitely conducting earth-image theory techniques can be utilized at any range from the source. Mohsen[5] has validated and extended these results to include higher order terms that correspond to multiple images at the same location. Mahmoud and Metwally,[6] employing discrete and discrete-plus-continuous images, have computed satisfactorily the change in the input impedance of a vertical magnetic dipole (VMD) due to the presence of the earth.

It is the purpose of this report to show that nearfield and farfield range finitely conducting earth-image theory techniques also can be employed for determining the fields produced by horizontal electric dipole (HED) and horizontal magnetic dipole (HMD) antennas (which are a combination of vertically and horizontally polarized sources).

In this report, the HED and HMD are situated at height h with respect to a cylindrical coordinate system (ρ,ϕ,z) and are assumed to carry a constant current I. The HED (of infinitesimal length ℓ) is oriented in the x direction while the axis of the HMD (of infinitesimal area A) is oriented in the y direction. The earth, which is assumed to be a homogeneous medium with conductivity σ_1 and dielectric constant $\varepsilon_1 (= \varepsilon_r \varepsilon_0)$, occupies the lower half-space $(z < 0)$ and the air occupies the upper half-space $(z > 0)$. The magnetic permeability of the earth is assumed to equal μ_0, the permeability of free space. Meter-kilogram-second (MKS) units are employed and a suppressed time factor of $\exp(i\omega t)$ is assumed.

LOCATION OF IMAGE DEPTH

Basic antenna theory tells us that the fields produced by a current-carrying wire of any length, when placed over a perfectly conducting earth, can be represented by the combined fields of the wire and its image.[7] If the finitely conducting earth could be replaced with a perfectly conducting earth at some specified depth below the surface of the finitely conducting earth, we then could use standard image theory to locate the antenna image and the resulting fields.

Several methods are available for deriving the depth of a perfectly conducting plane that can be used to replace a finitely conducting earth. One of the most general methods[8] is to equate the wave impedances for grazing incidence at the surface $(z = 0)$ for the two cases shown in figure 2.

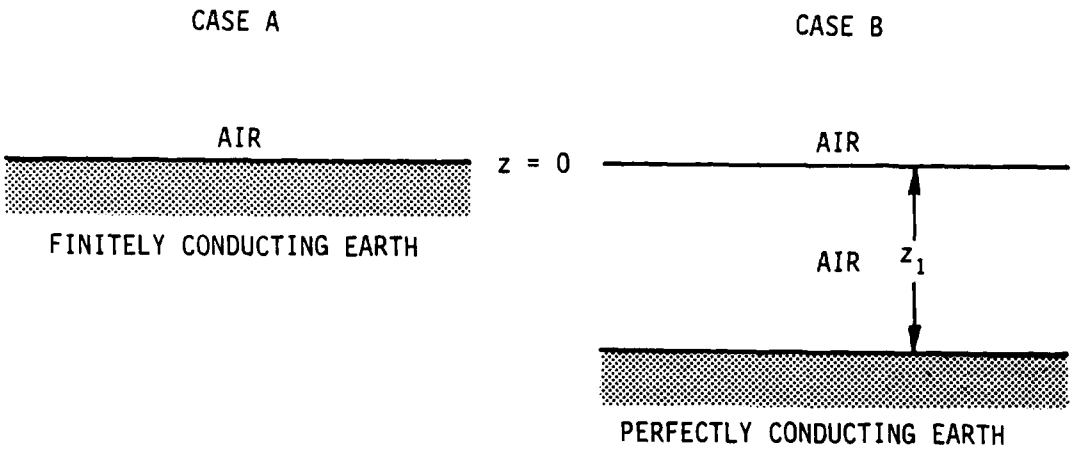

Figure 2. Replacement of a Finitely Conducting Earth With a Perfectly Conducting Earth at Depth z_1

For case A, for transverse electric (TE) propagation,

$$Z_A = \frac{\eta_1}{\sqrt{1 - \gamma_0^2/\gamma_1^2}} , \tag{1}$$

where $\gamma_0^2 = -\omega^2\mu_0\varepsilon_0$, $\gamma_1^2 = i\omega\mu_0(\sigma_1 + i\omega\varepsilon_1)$, and

$$\eta_1 = \left(\frac{i\omega\mu_0}{\sigma_1 + i\omega\varepsilon_1}\right)^{1/2} . \tag{2}$$

For case B, we can write

$$Z_B \sim \eta_0 \tanh(\gamma_0 z_1) , \tag{3}$$

where $\eta_0 = \sqrt{\mu_0/\varepsilon_0} \sim 120\pi$.

For small values of z_1 (i.e., $|\gamma_0 z_1| \leq 0.5$), $\tanh(\gamma_0 z_1) \sim \gamma_0 z_1$, and

$$Z_B \sim \eta_0\gamma_0 z_1 = i\omega\mu_0 z_1 . \tag{4}$$

Equating the two impedances results in

$$z_1 \sim \frac{1}{\gamma_1\sqrt{1 - \gamma_0^2/\gamma_1^2}} = \frac{1}{\sqrt{\gamma_1^2 - \gamma_0^2}} . \tag{5}$$

Since the image depth is equal to $2z_1$, we see that, for TE propagation, the image depth d_{TE} for a wire on the surface of a finitely conducting earth can be expressed as

$$d_{TE} \sim \frac{2}{\sqrt{\gamma_1^2 - \gamma_0^2}} = \frac{2/\gamma_1}{\sqrt{1 - 1/n^2}} , \tag{6}$$

subject to the condition that $|\gamma_0 z_1| \leq 0.5$ (i.e., $|\sqrt{n^2 - 1}| \geq 2$, where $n^2 = \gamma_1^2/\gamma_0^2$).

Similarly, for transverse magnetic (TM) propagation, since

$$Z_A = \eta_1 \sqrt{1 - \gamma_0^2/\gamma_1^2} , \tag{7}$$

then,

$$d_{TM} \sim \frac{2}{\gamma_1}\sqrt{1 - \gamma_0^2/\gamma_1^2} = \frac{2}{\gamma_1}\sqrt{1 - 1/n^2} , \tag{8}$$

subject to the condition that $|\gamma_0 z_1| \leq 0.5$ (i.e., $|n^2/\sqrt{n^2 - 1}| \geq 2$).

For normal incidence, or if $|n^2| > 15$, equations (6) and (8) reduce to the well-known result[1,2,3,8]

$$d_{TE} \sim d_{TM} \sim d \sim 2/\gamma_1 , \tag{9}$$

where $\gamma_1 \sim \sqrt{i\omega\mu_0\sigma_1}$ for $\sigma_1 >> \omega\varepsilon_0\varepsilon_r$ and $\gamma_1 \sim 60\pi\sigma_1/\sqrt{\varepsilon_r} + i\omega\sqrt{\mu_0\varepsilon_0\varepsilon_r}$ for $\sigma_1 << \omega\varepsilon_0\varepsilon_r$.

Another way to determine the finitely conducting earth-image depth is to compare the results obtained from image theory with known analytical results. For $z = h = 0$, the HED Hertz vector is exactly equal to[9]

$$\Pi_x \equiv \frac{I\ell}{4\pi i\omega\varepsilon_0} \times \frac{2}{(\gamma_1^2 - \gamma_0^2)\rho^3}\left[(1 + \gamma_0\rho)e^{-\gamma_0\rho} - (1 + \gamma_1\rho)e^{-\gamma_1\rho}\right] . \tag{10}$$

The image-theory result is

$$\Pi_x \sim \frac{I\ell}{4\pi i\omega\varepsilon_0}\left[\frac{e^{-\gamma_0\rho}}{\rho} - \frac{e^{-\gamma_0\rho_i}}{\rho_i}\right] , \tag{11}$$

where

$$\rho_i = \left(\rho^2 + d_{TE}^2\right)^{1/2} .$$

When $\mathrm{Re}\gamma_1\rho >> 1$, equation (10) reduces to

$$\Pi_x \sim \frac{I\ell}{4\pi i\omega\varepsilon_0\rho^3}\left(\frac{2}{\gamma_1^2 - \gamma_0^2}\right)(1 + \gamma_0\rho)e^{-\gamma_0\rho} , \tag{12}$$

while equation (11) becomes

$$\Pi_x \sim \frac{I\ell}{4\pi i\omega\varepsilon_0\rho^3}\left(\frac{d_{TE}^2}{2}\right)(1 + \gamma_0\rho)e^{-\gamma_0\rho} . \tag{13}$$

Equating equations (12) and (13) results in

$$d_{TE} \sim \frac{2}{\sqrt{\gamma_1^2 - \gamma_0^2}} , \tag{14}$$

which is identical to equation (6).

Following Wait and Spies,[3] another way to determine the image depth is to expand the function

$$f(u_0) = e^{u_0 d}\left(\frac{u_1 - u_0}{u_1 + u_0}\right) \tag{15}$$

in a Taylor series about $u_0 = 0$, resulting in

$$\frac{u_1 - u_0}{u_1 + u_0} \sim e^{-u_0 d}\left[1 + \frac{1}{3}\left(\frac{u_0 d}{2}\right)^3 + \cdots\right] , \tag{16}$$

where d is given by equation (6).

The introduction of $\exp(-u_0 d)$ into the Π_x integral equation yields an image at a distance h + d from the earth's surface (see figure 1), while higher order terms would correspond to multiple images at the same location.[5,6]

HED AIR-TO-AIR PROPAGATION

When h and z are ≥ 0, the Sommerfeld integral expressions for the HED Hertz vector are[9-11]

$$\Pi_x = \frac{I\ell}{4\pi i\omega\varepsilon_0}\left\{\frac{e^{-\gamma_0 R_0}}{R_0} - \frac{e^{-\gamma_0 R_1}}{R_1} + \int_0^\infty \left(\frac{2u_0}{u_1 + u_0}\right)e^{-u_0(z+h)} J_0(\lambda\rho)\frac{\lambda}{u_0}d\lambda\right\} \tag{17}$$

and

$$\Pi_z = \frac{I\ell\cos\phi}{4\pi i\omega\varepsilon_0} \times \frac{\partial}{\partial\rho}\int_0^\infty \frac{2(u_1 - u_0)}{\gamma_1^2 u_0 + \gamma_0^2 u_1} e^{-u_0(z+h)} J_0(\lambda\rho)\lambda d\lambda , \tag{18}$$

where $R_0^2 = \rho^2 + (z - h)^2$, $R_1^2 = \rho^2 + (z + h)^2$, $u_0^2 = \lambda^2 + \gamma_0^2$, and $u_1^2 = \lambda^2 + \gamma_1^2$.

From equations (17) and (18),

$$\vec{\nabla} \cdot \vec{\Pi} = \frac{I\ell \cos \phi}{4\pi i\omega\varepsilon_0} \times \frac{\partial}{\partial\rho}\left\{\frac{e^{-\gamma_0 R_0}}{R_0} - \frac{e^{-\gamma_0 R_1}}{R_1} + \int_0^\infty \frac{2\gamma_0^2 e^{-u_0(z+h)}}{\gamma_1^2 u_0 + \gamma_0^2 u_1} J_0(\lambda\rho)\lambda d\lambda\right\}. \quad (19)$$

If $|\gamma_0 z_1| \leq 0.5$ (i.e., $|\sqrt{n^2 - 1}| \geq 2$), which is applicable in most practical cases (for example, $|n^2| \geq 81$ at all frequencies for the sea/air case),

$$\frac{u_1 - u_0}{u_1 + u_0} \sim e^{-u_0 d} \quad (20)$$

and

$$1 - \left(\frac{u_1 - u_0}{u_1 + u_0}\right) = \frac{2u_0}{u_1 + u_0} \sim 1 - e^{-u_0 d} . \quad (21)$$

For small Sommerfeld numerical distances (i.e., $|\gamma_0 R_1 \sqrt{n^2 - 1}/(2n^3)| << 1$),

$$\gamma_1^2 u_0 + \gamma_0^2 u_1 \sim \gamma_1^2 u_0 . \quad (22)$$

Utilization of the identity $(u_1 - u_0)(u_1 + u_0) = \gamma_1^2 - \gamma_0^2$, equations (21) and (22), and Sommerfeld's integral[10]

$$P = \int_0^\infty e^{-u_0(z+h)} J_0(\lambda\rho)\frac{\lambda}{u_0} d\lambda = \frac{e^{-\gamma_0 R_1}}{R_1} , \quad (23)$$

results in

$$\Pi_x \sim \frac{I\ell}{4\pi i\omega\varepsilon_0}\left\{\frac{e^{-\gamma_0 R_0}}{R_0} - \frac{e^{-\gamma_0 R_1}}{R_1} + \frac{e^{-\gamma_0 R_1}}{R_1} - \frac{e^{-\gamma_0 R_2}}{R_2}\right\} - \frac{I\ell}{4\pi i\omega\varepsilon_0}\left\{\frac{e^{-\gamma_0 R_0}}{R_0} - \frac{e^{-\gamma_0 R_2}}{R_2}\right\} \quad (24)$$

$$\vec{\nabla} \cdot \vec{\Pi} \sim \frac{I\ell \cos \phi}{4\pi i\omega\varepsilon_0} \times \frac{\partial}{\partial\rho}\left\{\frac{e^{-\gamma_0 R_0}}{R_0} - \left(1 - \frac{2}{n^2}\right)\frac{e^{-\gamma_0 R_1}}{R_1}\right\} \sim -\frac{I\ell\rho \cos \phi}{4\pi i\omega\varepsilon_0}\left\{(1 + \gamma_0 R_0)\frac{e^{-\gamma_0 R_0}}{R_0^3} - \left(1 - \frac{2}{n^2}\right)(1 + \gamma_0 R_1)\frac{e^{-\gamma_0 R_1}}{R_1^3}\right\} \quad (25)$$

and

$$\Pi_z \sim \frac{I\ell \cos\phi}{4\pi i\omega\varepsilon_0}(1 - 1/n^2)\frac{\partial}{\partial\rho}\int_0^\infty \left(1 - e^{-u_0 d}\right)e^{-u_0(z+h)}J_0(\lambda\rho)\frac{\lambda}{u_0^2}d\lambda$$

$$= -\frac{I\ell \cos\phi}{4\pi i\omega\varepsilon_0}(1 - 1/n^2)\int_0^\infty \left(1 - e^{-u_0 d}\right)e^{-u_0(z+h)}J_1(\lambda\rho)\frac{\lambda^2}{u_0^2}d\lambda \ , \tag{26}$$

where $R_2^2 = \rho^2 + (d + z + h)^2$.

Because of the u_0^2 term in the denominator of equation (26), it does not readily appear that the equation can be expressed in closed form, except for the quasi-static range ($\gamma_0 \sim 0$), where equation (26) reduces to

$$\Pi_z \sim -\frac{I\ell \cos\phi}{4\pi i\omega\varepsilon_0}\int_0^\infty \left(1 - e^{-\lambda d}\right)e^{-\lambda(z+h)}J_1(\lambda\rho)d\lambda$$

$$= -\frac{I\ell \cos\phi}{4\pi i\omega\varepsilon_0\rho}\left\{\frac{(d + z + h)}{R_2} - \frac{(z + h)}{R_1}\right\}, \tag{27}$$

However, if we replace λ^2 by $u_0^2 - \gamma_0^2$, equation (26) can be broken up nto four integrals, two of which are of the type

$$\int_0^\infty e^{-u_0 z}J_1(\lambda\rho)d\lambda = \frac{1}{\rho}\left\{e^{-\gamma_0 z} - \frac{z}{R}e^{-\gamma_0 R}\right\} \ , \tag{28}$$

where $R^2 = \rho^2 + z^2$, and two of which are of the type

$$\gamma_0^2\int_0^\infty \frac{e^{-u_0 z}}{u_0^2}J_1(\lambda\rho)d\lambda \ . \tag{29}$$

Since[12]

$$\int_0^\infty \frac{e^{-u_0 z}}{u_0}J_1(\lambda\rho)d\lambda = \frac{1}{\gamma_0\rho}\left\{e^{-\gamma_0 z} - e^{-\gamma_0 R}\right\} \ , \tag{30}$$

then

$$\gamma_0^2 \int_0^\infty \frac{e^{-u_0 z}}{u_0^2} J_1(\lambda\rho)\,d\lambda = \frac{e^{-\gamma_0 z}}{\rho} + \frac{\gamma_0}{\rho}\int_z e^{-\gamma_0 R}\,dz \ . \tag{31}$$

Inserting equations (28) and (31) into equation (26) results in

$$\Pi_z \sim -\frac{I\ell \cos\phi(1 - 1/n^2)}{4\pi i\omega\varepsilon_0\rho}\left\{\frac{(d + z + h)}{R_2}e^{-\gamma_0 R_2} - \frac{(z + h)}{R_1}e^{-\gamma_0 R_1} + I\right\} , \tag{32}$$

where

$$I = -\gamma_0 \int_z e^{-\gamma_0 R_1}\left[1 - e^{-\gamma_0 (R_2 - R_1)}\right] dz \ . \tag{33}$$

When $(z + h) >> \rho$, $R_1 \sim (z + h)$, and $R_2 - R_1 \sim d$, resulting in

$$I \sim \left(1 - e^{-\gamma_0 d}\right)e^{-\gamma_0 (z+h)} \ . \tag{34}$$

For $|\gamma_0 d| < 0.5$ (i.e., $|n^2| > 15$),

$$I \sim \gamma_0 d e^{-\gamma_0 (z+h)} \ . \tag{35}$$

Comparing equations (27) and (32), we see that for the quasi-static range ($|\gamma_0 R_1| << 1$), I is negligible compared to the other two terms in equation (32). Therefore, if we assume from the outset that $R_1 >> |d|$, equation (33) becomes

$$I \sim \gamma_0 d e^{-\gamma_0 R_1} \ , \tag{36}$$

which is identical to equation (35) when $(z + h) >> \rho$.

Therefore, we can approximate the HED Π_z vector as

$$\Pi_z \sim -\frac{I\ell \cos\phi(1 - 1/n^2)}{4\pi i\omega\varepsilon_0\rho}\left\{\frac{(d + z + h)e^{-\gamma_0 R_2}}{R_2} - \frac{(z + h)e^{-\gamma_0 R_1}}{R_1} + \gamma_0 d e^{-\gamma_0 R_1}\right\} , \tag{37}$$

subject to the restriction $|n^2| > 15$. This equation should also be valid for $|n^2| > 5$ if $\gamma_0 d$ is replaced by $\left(1 - e^{-\gamma_0 d}\right)$.

Now, it seems that we have gone to a lot of trouble to derive the last term of the Π_z expression. However, it is this term that yields the vertically polarized farfield (for small numerical distances) produced by a HED located

very near or below the earth's surface. This is the so-called quadripole term (i.e., the quadripole moment is $I\ell\gamma_0 d = 2I\ell/n$). Because of the close spacing and opposite sense of the dipole and its image, direct radiation from the dipole is not the prime mechanism. Rather, the quadripole consisting of vertical conduction currents in the lossy medium represents the prime source.[13]

If the first two terms in equation (37) are ignored and $z = h = 0$, equation (37) reduces to

$$\Pi_z \sim -\frac{I\ell \cos\phi}{4\pi i\omega\varepsilon_0\rho}\left(\gamma_0 d e^{-\gamma_0\rho}\right) . \tag{38}$$

When $|\gamma_0\rho| >> 1$,

$$H_\phi \sim -i\omega\varepsilon_0\frac{\partial\Pi_z}{\partial\rho} \sim -\frac{I\ell \cos\phi}{2\pi\gamma_1\rho}\left(\gamma_0^2\right)e^{-\gamma_0\rho} , \tag{39}$$

which is the correct farfield result for small numerical distances when $|n^2| >> 1$.

Since we have now derived expressions for the HED Hertz vector (equations (24), (25) and (37)), the fields in air can be obtained from

$$\begin{aligned} \vec{E} &= -\gamma_0^2\vec{\Pi} + \vec{\nabla}(\vec{\nabla}\cdot\vec{\Pi}) \\ H &= i\omega\varepsilon_0(\vec{\nabla}\times\vec{\Pi}) . \end{aligned} \tag{40}$$

The resulting HED finitely conducting earth-image theory field expressions for the air-to-air propagation case are presented in table 1. They are valid for small numerical distances and $|n^2| > 15$. When $|\gamma_0 R_1| << 1$, they reduce to the quasi-static range image-theory results.[1,2] When $|\gamma_0 R_1| >> 1$, they reduce to Norton's[14,15] farfield results.

These results easily can be extended to a multilayered earth simply by letting $d = (2/\gamma_1)Q$, where Q is the familiar plane-wave correction factor employed to account for the presence of stratification in the earth.[16,17]

HMD AIR-TO-AIR PROPAGATION

Four of the six HMD expressions valid for h and $z \geq 0$ can be obtained completely from reciprocity consideration (E_ρ, E_ϕ, E_z, and H_z). The remaining two can be obtained from Maxwell's equations (H_ρ and H_ϕ). Alternatively, they can be obtained from

Table 1. HED Air-to-Air Propagation Equations.

$$E_\rho \sim \frac{I\ell \cos\phi}{4\pi i\omega\varepsilon_0}\left\{\left[\left(\frac{3\rho^2}{R_0^2} - 1\right)(1 + \gamma_0 R_0) + \gamma_0^2\rho^2\right]\frac{e^{-\gamma_0 R_0}}{R_0^3} - \left[1 - \frac{2}{n^2}\right]\left[\left(\frac{3\rho^2}{R_1^2} - 1\right)\right.\right.$$

$$\left.\left. \cdot\ (1 + \gamma_0 R_1) + \gamma_0^2\rho^2\right]\frac{e^{-\gamma_0 R_1}}{R_1^3} - \gamma_0^2\left[\frac{e^{-\gamma_0 R_0}}{R_0} - \frac{e^{-\gamma_0 R_2}}{R_2}\right]\right\}$$

$$E_\phi \sim \frac{I\ell \sin\phi}{4\pi i\omega\varepsilon_0}\left\{(1 + \gamma_0 R_0)\frac{e^{-\gamma_0 R_0}}{R_0^3} - \left(1 - \frac{2}{n^2}\right)(1 + \gamma_0 R_1)\frac{e^{-\gamma_0 R_1}}{R_1^3}\right.$$

$$\left. + \gamma_0^2\left(\frac{e^{-\gamma_0 R_0}}{R_0} - \frac{e^{-\gamma_0 R_2}}{R_2}\right)\right\}$$

$$E_z \sim \frac{I\ell\rho \cos\phi}{4\pi i\omega\varepsilon_0}\left\{\frac{(z - h)}{R_0^5}\left(3 + 3\gamma_0 R_0 + \gamma_0^2 R_0^2\right)e^{-\gamma_0 R_0}\right.$$

$$- \left(1 - \frac{2}{n^2}\right)\frac{(z + h)}{R_1^5}\left(3 + 3\gamma_0 R_1 + \gamma_0^2 R_1^2\right)e^{-\gamma_0 R_1}$$

$$\left. + \frac{\gamma_0^2}{\rho^2}\left[\frac{(d + z + h)}{R_2}e^{-\gamma_0 R_2} + \frac{\gamma_0 d R_1 - (z + h)}{R_1}e^{-\gamma_0 R_1}\right]\right\}$$

$$H_\rho \sim \frac{I\ell \sin\phi}{4\pi}\left\{\frac{(d + z + h)}{R_2}\left[\frac{1}{\rho^2} + \frac{1}{R_2^2}(1 + \gamma_0 R_2)\right]e^{-\gamma_0 R_2}\right.$$

$$\left. + \left[\frac{\gamma_0 d R_1 - (z + h)}{\rho^2 R_1}\right]e^{-\gamma_0 R_1} - \frac{(z - h)}{R_0^3}(1 + \gamma_0 R_0)e^{-\gamma_0 R_0}\right\}$$

$$H_\phi \sim -\frac{I\ell \cos\phi}{4\pi}\left\{\frac{(z - h)}{R_0^3}(1 + \gamma_0 R_0)e^{-\gamma_0 R_0} - \frac{(z + h)}{R_1^3}(1 + \gamma_0 R_1)e^{-\gamma_0 R_1}\right.$$

$$\left. + \frac{1}{\rho^2}\left[\frac{(d + z + h)}{R_2}e^{-\gamma_0 R_2} - \frac{(z + h)}{R_1}e^{-\gamma_0 R_1}\right] + \frac{de^{-\gamma_0 R_1}}{\rho^2 R_1}\left[\gamma_0 R_1 + \gamma_0^2\rho^2\right]\right\}$$

$$H_z \sim \frac{I\ell\rho \sin\phi}{4\pi}\left\{(1 + \gamma_0 R_0)\frac{e^{-\gamma_0 R_0}}{R_0^3} - (1 + \gamma_0 R_2)\frac{e^{-\gamma_0 R_2}}{R_2^3}\right\}$$

$$H_\rho = -\gamma_0^2 \Pi_y \sin\phi + \frac{\partial}{\partial\rho}(\vec{\nabla} \cdot \vec{\Pi})$$

$$H_\phi = -\gamma_0^2 \Pi_y \cos\phi + \frac{1}{\rho} \times \frac{\partial}{\partial\phi}(\vec{\nabla} \cdot \vec{\Pi}) \quad . \tag{41}$$

Following the same procedure outlined in the derivation of the HED field components results in

$$\Pi_y \sim \frac{IA}{4\pi}\left\{\frac{e^{-\gamma_0 R_0}}{R_0} + \frac{e^{-\gamma_0 R_1}}{R_1}\right\} \tag{42}$$

and

$$\vec{\nabla} \cdot \vec{\Pi} \sim -\frac{IA\rho \sin\phi}{4\pi}\left\{\frac{e^{-\gamma_0 R_0}}{R_0^3}(1 + \gamma_0 R_0) + \frac{e^{-\gamma_0 R_2}}{R_2^3}(1 + \gamma_0 R_2)\right\} \quad . \tag{43}$$

The resulting HMD finitely conducting earth-image theory field expressions for the air-to-air propagation case are presented in table 2. They are valid for $|n^2| > 15$ and small numerical distances. When $|\gamma_0 R_1| << 1$, they reduce to the quasi-static range image-theory results.[1,2] When $|\gamma_0 R_1| >> 1$, they reduce to Norton's[14,15] farfield results.

SUBSURFACE-TO-AIR PROPAGATION

The HED and HMD image-theory expressions for the subsurface-to-air propagation case ($h \leq 0$, $z \geq 0$) can be obtained from the air-to-air propagation equations (tables 1 and 2) simply by setting $h = 0$ and multiplying each expression by $\exp(\gamma_1 h)$. The resulting equations are presented in tables 3 and 4 and will be valid[18] for $R = \sqrt{\rho^2 + z^2} > |3h|$, $|n^2| > 15$, and small numerical distances. It should be noted that by following the procedure outlined by Bannister and Dube,[18] the restriction $R > |3h|$ can become less stringent.

When $|\gamma_1 R| >> 1$, the HED and HMD subsurface-to-air propagation equations reduce to the nearfield and farfield range results presented in tables 3.1 and 3.3 of Kraichman[19] (see also Bannister[2]).

AIR-TO-SUBSURFACE PROPAGATION

The HED and HMD image-theory expressions for the air-to-subsurface propagation case ($h \geq 0$, $z \leq 0$) can be obtained from the air-to-air propagation equations (tables 1 and 2) simply by setting $z = 0$ and multiplying each expression by $\exp(\gamma_1 z)$. (Both E_z components must also be multiplied by $1/n^2$ to satisfy the boundary conditions.) The resulting equations are presented in tables 5 and 6 and will be valid[18] for $R' = \sqrt{\rho^2 + h^2} > |3z|$, $|n^2| > 15$, and small numerical distances.

Table 2. HMD Air-to-Air Propagation Equations

$$E_\rho \sim -\frac{i\omega\mu_0 IA\cos\phi}{4\pi}\left\{\frac{(z-h)}{R_0^3}(1+\gamma_0R_0)e^{-\gamma_0R_0}+\frac{(z+h)}{R_1^3}(1+\gamma_0R_1)e^{-\gamma_0R_1}\right.$$
$$\left.-\frac{1}{\rho^2}\left[\frac{(d+z+h)}{R_2}e^{-\gamma_0R_2}-\frac{(z+h)}{R_1}e^{-\gamma_0R_1}\right]-\frac{de^{-\gamma_0R_1}}{\rho^2R_1}(\gamma_0R_1+\gamma_0^2\rho^2)\right\}$$

$$E_\rho \sim \frac{i\omega\mu_0 IA\sin\phi}{4\pi}\left\{\frac{(d+z+h)}{R_2}\left[\frac{1}{\rho^2}+\frac{1}{R_2^2}(1+\gamma_0R_2)\right]e^{-\gamma_0R_2}\right.$$
$$\left.+\left[\frac{\gamma_0dR_1-(z+h)}{\rho^2R_1}\right]e^{-\gamma_0R_1}+\frac{(z-h)}{R_0^3}(1+\gamma_0R_0)e^{-\gamma_0R_0}\right\}$$

$$E_z \sim \frac{i\omega\mu_0 IA\rho\cos\phi}{4\pi}\left\{(1+\gamma_0R_0)\frac{e^{-\gamma_0R_0}}{R_0^3}+(1+\gamma_0R_1)\frac{e^{-\gamma_0R_1}}{R_1^3}\right\}$$

$$H_\rho \sim \frac{IA\sin\phi}{4\pi}\left[\left\{\left[2-\frac{3(z-h)^2}{R_0^2}\right]\left[1+\gamma_0R_0\right]-\gamma_0^2(z-h)^2\right\}\frac{e^{-\gamma_0R_0}}{R_0^3}\right.$$
$$\left.+\left\{\left[2-\frac{3(d+z+h)^2}{R_2^2}\right]\left[1+\gamma_0R_2\right]+\gamma_0^2\rho^2\right\}\frac{e^{-\gamma_0R_2}}{R_2^3}-\frac{\gamma_0^2R_1^2e^{-\gamma_0R_1}}{R_1^3}\right]$$

$$H_\phi \sim -\frac{IA\cos\phi}{4\pi}\left\{(1+\gamma_0R_0+\gamma_0^2R_0^2)\frac{e^{-\gamma_0R_0}}{R_0^3}\right.$$
$$\left.+(1+\gamma_0R_2)\frac{e^{-\gamma_0R_2}}{R_2^3}+\gamma_0^2R_1^2\frac{e^{-\gamma_0R_1}}{R_1^3}\right\}$$

$$H_z \sim \frac{IA\rho\sin\phi}{4\pi}\left\{\frac{(d+z+h)e^{-\gamma_0R_2}}{R_2^5}(3+3\gamma_0R_2+\gamma_0^2R_2^2)\right.$$
$$\left.+\frac{(z-h)e^{-\gamma_0R_0}}{R_0^5}(3+3\gamma_0R_0+\gamma_0^2R_0^2)\right\}$$

Table 3. HED Subsurface-to-Air Propagation Equations
$[R^2 = \rho^2 + z^2,\ R_i^2 = \rho^2 + (d + z)^2]$.

$$E_\rho \sim \frac{I\ell \cos\phi e^{-(\gamma_0 R - \gamma_1 h)}}{2\pi(\sigma_1 + i\omega\epsilon_1)R^3}\left\{\left(\frac{3\rho^2}{R^2} - 1\right)(1 + \gamma_0 R) + \gamma_0^2\rho^2 - \frac{2R^2}{d^2}\left[1 - \frac{R}{R_i}e^{-\gamma_0(R_i - R)}\right]\right\}$$

$$E_\phi \sim \frac{I\ell \sin\phi e^{-(\gamma_0 R - \gamma_1 h)}}{2\pi(\sigma_1 + i\omega\epsilon_1)R^3}\left\{(1 + \gamma_0 R) + \frac{2R^2}{d^2}\left[1 - \frac{R}{R_i}e^{-\gamma_0(R_i - R)}\right]\right\}$$

$$E_z \sim \frac{I\ell i\omega\mu_0 \cos\phi e^{-(\gamma_0 R - \gamma_1 h)}}{4\pi\rho R}\left\{\gamma_0 Rd - z + \frac{R}{R_i}(d + z)e^{-\gamma_0(R_i - R)} + \frac{\rho^2 d^2 z}{2R^4}\left(3 + 3\gamma_0 R + \gamma_0^2 R^2\right)\right\}$$

$$H_\rho \sim \frac{I\ell \sin\phi e^{-(\gamma_0 R - \gamma_1 h)}}{4\pi\rho^2 R}\left\{\gamma_0 Rd - z\left[1 + \frac{\rho^2}{R^2}(1 + \gamma_0 R)\right] + (d + z)\frac{R}{R_i}e^{-\gamma_0(R_i - R)}\left[1 + \frac{\rho^2}{R_i^2}(1 + \gamma_0 R_i)\right]\right\}$$

$$H_\phi \sim -\frac{I\ell \cos\phi e^{-(\gamma_0 R - \gamma_1 h)}}{4\pi\rho^2 R}\left\{d\left(\gamma_0 R + \gamma_0^2\rho^2\right) - z + \frac{R}{R_i}(d + z)e^{-\gamma_0(R_i - R)}\right\}$$

$$H_z \sim \frac{I\ell\rho \sin\phi e^{-(\gamma_0 R - \gamma_1 h)}}{4\pi R^3}\left\{(1 + \gamma_0 R) - \frac{R^3}{R_i^3}(1 + \gamma_0 R_i)e^{-\gamma_0(R_i - R)}\right\}$$

Table 4. HMD Subsurface-to-Air Propagation Equations
$[R^2 = \rho^2 + z^2,\ R_i^2 = \rho^2 + (d + z)^2]$

$$E_\rho \sim \frac{i\omega\mu_0 IA \cos\phi}{4\pi\rho^2 R} e^{-(\gamma_0 R - \gamma_1 h)} \left\{ d\left(\gamma_0 R + \gamma_0^2\rho^2\right) - \frac{2z\rho^2}{R^2}(1 + \gamma_0 R) + (d + z)\frac{R}{R_i} e^{-\gamma_0(R_i - R)} - z \right\}$$

$$E_\phi \sim \frac{i\omega\mu_0 IA \sin\phi}{4\pi\rho^2 R} e^{-(\gamma_0 R - \gamma_1 h)} \left\{ d\gamma_0 R - z + \frac{\rho^2 z}{R^2}(1 + \gamma_0 R) + (d + z)\frac{R}{R_i}\left[1 + \frac{\rho^2}{R_i^2}(1 + \gamma_0 R_i)\right] e^{-\gamma_0(R_i - R)} \right\}$$

$$E_z \sim \frac{i\omega\mu_0 IA\rho \cos\phi}{2\pi R^3}(1 + \gamma_0 R) e^{-(\gamma_0 R - \gamma_1 h)}$$

$$H_\rho \sim \frac{IA \sin\phi}{4\pi R^3} e^{-(\gamma_0 R - \gamma_1 h)} \left[\left(2 - \frac{3z^2}{R^2}\right)(1 + \gamma_0 R) - 2\gamma_0^2 z^2 - \gamma_0^2\rho^2 + \left(\frac{R}{R_i}\right)^3 e^{-\gamma_0(R_i - R)} \left\{ \left[2 - \frac{3(d + z)^2}{R_i^2} \right] \left[1 + \gamma_0 R_i \right] + \gamma_0^2\rho^2 \right\} \right]$$

$$H_\phi \sim -\frac{IA \cos\phi}{4\pi R^3} e^{-(\gamma_0 R - \gamma_1 h)} \left\{ 1 + \gamma_0 R + 2\gamma_0^2 R^2 + \left(\frac{R}{R_i}\right)^3 (1 + \gamma_0 R_i) e^{-\gamma_0(R_i - R)} \right\}$$

$$H_z \sim \frac{IA\rho \sin\phi}{4\pi R^5} e^{-(\gamma_0 R - \gamma_1 h)} \left\{ z\left(3 + 3\gamma_0 R + \gamma_0^2 R^2\right) + (d + z)\left(\frac{R}{R_i}\right)^5 \left(3 + 3\gamma_0 R_i + \gamma_0^2 R_i^2\right) e^{-\gamma_0(R_i - R)} \right\}$$

Table 5. HED Air-to-Subsurface Propagation Equations
$[(R')^2 = \rho^2 + h^2,\ (R_i')^2 = \rho^2 + (d + h)^2]$

$$E_\rho \sim \frac{I\ell \cos\phi e^{-(\gamma_0 R' - \gamma_1 z)}}{2\pi(\sigma_1 + i\omega\varepsilon_1)(R')^3}\left\{\left[\frac{3\rho^2}{(R')^2} - 1\right]\left[1 + \gamma_0 R'\right] + \gamma_0^2\rho^2 - \frac{2(R')^2}{d^2}\left[1 - \frac{R'}{R_i'}e^{-\gamma_0(R_i' - R')}\right]\right\}$$

$$E_\phi \sim \frac{I\ell \sin\phi e^{-(\gamma_0 R' - \gamma_1 z)}}{2\pi(\sigma_1 + i\omega\varepsilon_1)(R')^3}\left\{1 + \gamma_0 R' + \frac{2(R')^2}{d^2}\left[1 - \frac{R'}{R_i'}e^{-\gamma_0(R_i' - R')}\right]\right\}$$

$$E_z \sim -\frac{I\ell\rho \cos\phi e^{-(\gamma_0 R' - \gamma_1 z)}}{2\pi(\sigma_1 + i\omega\varepsilon_1)(R')^5}\left\{h\left[3 + 3\gamma_0 R' + \gamma_0^2(R')^2\right] - \frac{\gamma_0^2(R')^4}{2\rho^2}\left[\gamma_0 dR' - h + \frac{R'}{R_i'}(d + h)e^{-\gamma_0(R_i' - R')}\right]\right\}$$

$$H_\rho \sim \frac{I\ell \sin\phi e^{-(\gamma_0 R' - \gamma_1 z)}}{4\pi(R')^3}\left\{\frac{R'}{R_i'}(d + h)\left[\left(\frac{R'}{\rho}\right)^2 + \left(\frac{R'}{R_i'}\right)^2\left(1 + \gamma_0 R_i'\right)\right]e^{-\gamma_0(R_i' - R')} + h(1 + \gamma_0 R') + \left(\frac{R'}{\rho}\right)^2(d\gamma_0 R' - h)\right\}$$

$$H_\phi \sim -\frac{I\ell \cos\phi e^{-(\gamma_0 R' - \gamma_1 z)}}{4\pi(R')^3}\left\{\left(\frac{R'}{\rho}\right)^2\left[(d + h)\frac{R'}{R_i'}e^{-\gamma_0(R_i' - R')} + d\left(\gamma_0 R' + \gamma_0^2\rho^2\right) - h\right] - 2h\left(1 + \gamma_0 R'\right)\right\}$$

$$H_z \sim \frac{I\ell\rho \sin\phi e^{-(\gamma_0 R' - \gamma_1 z)}}{4\pi(R')^3}\left\{\left(1 + \gamma_0 R'\right) - \left(\frac{R'}{R_i'}\right)^3\left(1 + \gamma_0 R_i'\right)e^{-\gamma_0(R_i' - R')}\right\}$$

Table 6. HMD Air-to-Subsurface Propagation Equations
$[(R')^2 = \rho^2 + h^2,\ (R_i')^2 = \rho^2 + (d + h)^2]$

$$E_\rho \sim \frac{i\omega\mu_0 IA \cos\phi e^{-(\gamma_0 R' - \gamma_1 z)}}{4\pi\rho^2 R'} \left\{ (d + h)\frac{R'}{R_i'} e^{-\gamma_0 (R_i' - R')} - h + d\left(\gamma_0 R' + \gamma_0^2 \rho^2\right) \right\}$$

$$E_\phi \sim \frac{i\omega\mu_0 IA \sin\phi e^{-(\gamma_0 R' - \gamma_1 z)}}{4\pi\rho^2 R'} \left\{ \gamma_0 dR' - h - \frac{\rho^2 h}{(R')^2}(1 + \gamma_0 R') + (d + h)\frac{R'}{R_i'}\left[1 + \frac{\rho^2}{(R_i')^2}(1 + \gamma_0 R_i')\right] e^{-\gamma_0 (R_i' - R')} \right\}$$

$$E_z \sim \frac{i\omega\mu_0 IA\rho \cos\phi}{2\pi n^2 (R')^3}(1 + \gamma_0 R') e^{-(\gamma_0 R' - \gamma_1 z)}$$

$$H_\rho \sim \frac{IA \sin\phi e^{-(\gamma_0 R' - \gamma_1 z)}}{4\pi (R')^3} \left[\left\{ 2 - \frac{3h^2}{(R')^2} \right\} \left\{ 1 + \gamma_0 R' \right\} - 2\gamma_0^2 h^2 - \gamma_0^2 \rho^2 + \left\{ \left[2 - \frac{3(d + h)^2}{(R_i')^2} \right] \left[1 + \gamma_0 R_i' \right] + \gamma_0^2 \rho^2 \right\} \left(\frac{R'}{R_i'} \right)^3 e^{-\gamma_0 (R_i' - R')} \right]$$

$$H_\phi \sim - \frac{IA \cos\phi e^{-(\gamma_0 R' - \gamma_1 z)}}{4\pi (R')^3} \left\{ 1 + \gamma_0 R' + \gamma_0^2 (R')^2 + \left(\frac{R'}{R_i'} \right)^3 \left(1 + \gamma_0 R_i' \right) e^{-\gamma_0 (R_i' - R')} \right\}$$

$$H_z \sim \frac{IA\rho \sin\phi e^{-(\gamma_0 R' - \gamma_1 z)}}{4\pi (R')^5} \left\{ (d + h) \left(\frac{R'}{R_i'} \right)^5 \left[3 + 3\gamma_0 R_i' + \gamma_0^2 (R_i')^2 \right] e^{-\gamma_0 (R_i' - R')} - h \left[3 + 3\gamma_0 R' + \gamma_0^2 (R')^2 \right] \right\}$$

When $|\gamma_1 R'| >> 1$, the HED and HMD air-to-subsurface propagation equations reduce to the nearfield range results presented in table 3.5 of Kraichman.[19]

SUBSURFACE-TO-SUBSURFACE PROPAGATION

The HED and HMD image-theory expressions for the subsurface-to-subsurface propagation case ($h \leq 0$, $z \leq 0$) can be obtained from the air-to-air propagation equations (tables 1 and 2) simply by setting both z and h equal to zero and multiplying each expression by $\exp[\gamma_1(z + h)]$. (Both E_z components must also be multiplied by $1/n^2 = \gamma_0^2/\gamma_1^2$ to satisfy the boundary conditions.) The resulting expressions are presented in tables 7 and 8 and should be valid[18] (for most cases) for $\rho > 3|z + h|$, $|n^2| > 15$, and small numerical distances. When $|\gamma_0 \rho| << 1$ and $z = h = 0$, these expressions reduce to the quasi-static range surface-to-surface image-theory results.[1,2] When $|\gamma_1 \rho| >> 1$, they reduce to the subsurface-to-subsurface nearfield and farfield range results presented in tables 3.2 and 3.7 of Kraichman.[19]

COMPARISON WITH EXACT SOMMERFELD INTEGRATION RESULTS

Mittra et al.[20] have presented some exact Sommerfeld integration results for the HED ${}_0\Pi_x$ and Π_z vectors (i.e., the correction terms to the perfectly conducting ground solution) for frequencies of 3 to 30 MHz. For their case, $R_1 = 10$ m, $\theta = \tan^{-1}[\rho/(z + h)] = 10°$, $\phi = 0°$, and the quantity $I_0 = I\ell/(i\omega\varepsilon_0)$ is normalized to unity.

The image-theory solution of Π_z is given by equation (37), while ${}_0\Pi_x$ is given by the last two terms of equation (24); that is,

$$ {}_0\Pi_x \sim \frac{I_0}{4\pi}\left[\frac{e^{-\gamma_0 R_1}}{R_1} - \frac{e^{-\gamma_0 R_2}}{R_2}\right] . \tag{44}$$

A comparison of the image theory and exact Sommerfeld integration results for the situation where $\varepsilon_r = 40$ and $\sigma_1 = 1$ S/m is presented in figure 3. For this situation, n^2 varies from 40 - j150 at 3 MHz to 40 - j15 at 30 MHz. Since $|n^2| > 15$, $d_{TM} \sim d_{TE} \sim d = 2/\gamma_1$. Note that the agreement between the two solutions is excellent.

Presented in figure 4 is a comparison of the image-theory and exact Sommerfeld integration results for the case where $\varepsilon_r = 10$ and $\sigma_1 = 10^{-2}$ S/m. For this case, n^2 varies from 10 - j6 at 3 MHz to 10 - j0.6 at 30 MHz. Since $|n^2| < 15$ and $(z + h) >> \rho$, we have replaced $\gamma_0 d$ by $1 - \exp(-\gamma_0 d)$ in the image theory Π_z expression (equation (37)). Note that the agreement is excellent (within 1 percent for the ${}_0\Pi_x$ component and very good (within 5 percent) for the Π_z component.

Table 7. HED Subsurface-to-Subsurface Propagation Equations ($\rho_i^2 = \rho^2 + d^2$)

$$E_\rho \sim \frac{I\ell \cos\phi e^{-[\gamma_0\rho - \gamma_1(z+h)]}}{2\pi(\sigma_1 + i\omega\epsilon_1)\rho^3}\left\{2 + 2\gamma_0\rho + \gamma_0^2\rho^2 - \frac{2\rho^2}{d^2}\left[1 - \frac{\rho}{\rho_i}e^{-\gamma_0(\rho_i-\rho)}\right]\right\}$$

$$E_\phi \sim \frac{I\ell \sin\phi e^{-[\gamma_0\rho - \gamma_1(z+h)]}}{2\pi(\sigma_1 + i\omega\epsilon_1)\rho^3}\left\{1 + \gamma_0\rho + \frac{2\rho^2}{d^2}\left[1 - \frac{\rho}{\rho_i}e^{-\gamma_0(\rho_i-\rho)}\right]\right\}$$

$$E_z \sim \frac{I\ell\gamma_1 \cos\phi e^{-[\gamma_0\rho - \gamma_1(z+h)]}}{2\pi(\sigma_1 + i\omega\epsilon_1)n^2\rho^2}\left\{\gamma_0\rho + \frac{\rho}{\rho_i}e^{-\gamma_0(\rho_i-\rho)}\right\}$$

$$H_\rho \sim \frac{I\ell \sin\phi e^{-[\gamma_0\rho - \gamma_1(z+h)]}}{2\pi\gamma_1\rho^3}\left\{\frac{\rho}{\rho_i}\left[1 + \frac{\rho^2}{\rho_i^2}(1 + \gamma_0\rho_i)\right]e^{-\gamma_0(\rho_i-\rho)} + \gamma_0\rho\right\}$$

$$H_\phi \sim -\frac{I\ell \cos\phi e^{-[\gamma_0\rho - \gamma_1(z+h)]}}{2\pi\gamma_1\rho^3}\left\{\frac{\rho}{\rho_i}e^{-\gamma_0(\rho_i-\rho)} + \gamma_0\rho + \gamma_0^2\rho^2\right\}$$

$$H_z \sim \frac{I\ell \sin\phi e^{-[\gamma_0\rho - \gamma_1(z+h)]}}{4\pi\rho^2}\left\{(1 + \gamma_0\rho) - \frac{\rho^3}{\rho_i^3}(1 + \gamma_0\rho_i)e^{-\gamma_0(\rho_i-\rho)}\right\}$$

Table 8. HMD Subsurface-to-Subsurface Propagation Equations ($\rho_i^2 = \rho^2 + d^2$)

$$E_\rho \sim \frac{IA\gamma_1 \cos\phi e^{-[\gamma_0\rho-\gamma_1(z+h)]}}{2\pi(\sigma_1 + i\omega\varepsilon_1)\rho^3}\left\{\frac{\rho}{\rho_i}e^{-\gamma_0(\rho_i-\rho)} + \gamma_0\rho + \gamma_0^2\rho^2\right\}$$

$$E_\phi \sim \frac{IA\gamma_1 \sin\phi e^{-[\gamma_0\rho-\gamma_1(z+h)]}}{2\pi(\sigma_1 + i\omega\varepsilon_1)\rho^3}\left\{\frac{\rho}{\rho_i}\left[1 + \frac{\rho^2}{\rho_i^2}(1 + \gamma_0\rho_i)\right]e^{-\gamma_0(\rho_i-\rho)} + \gamma_0\rho\right\}$$

$$E_z \sim \frac{i\omega\mu_0 IA \cos\phi e^{-[\gamma_0\rho-\gamma_1(z+h)]}}{2\pi n^2\rho^2}(1 + \gamma_0\rho)$$

$$H_\rho \sim \frac{IA \sin\phi e^{-[\gamma_0\rho-\gamma_1(z+h)]}}{4\pi\rho^3}\left[2(1 + \gamma_0\rho) - \gamma_0^2\rho^2 + \left(\frac{\rho}{\rho_i}\right)^3 e^{-\gamma_0(\rho_i-\rho)}\left\{\left[2 - \frac{3d^2}{\rho_i^2}\right]\left[1 + \gamma_0\rho_i\right] + \gamma_0^2\rho^2\right\}\right]$$

$$H_\phi \sim -\frac{IA \cos\phi e^{-[\gamma_0\rho-\gamma_1(z+h)]}}{4\pi\rho^3}\left\{1 + \gamma_0\rho + 2\gamma_0^2\rho^2 + \left(\frac{\rho}{\rho_i}\right)^3(1 + \gamma_0\rho_i)e^{-\gamma_0(\rho_i-\rho)}\right\}$$

$$H_z \sim \frac{IA\rho \sin\phi e^{-[\gamma_0\rho_i-\gamma_1(z+h)]}}{2\pi\gamma_1\rho_i^5}\left(3 + 3\gamma_0\rho_i + \gamma_0^2\rho_i^2\right)$$

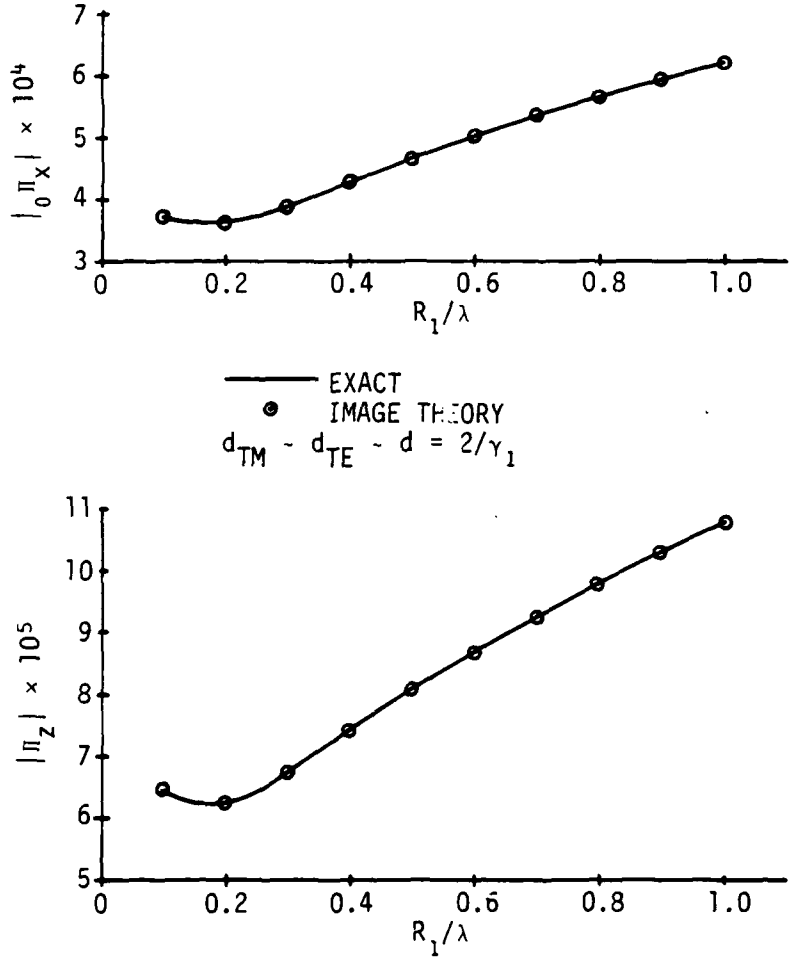

Figure 3. Comparison of Image-Theory and Exact Sommerfeld Integration Results for $\varepsilon_r = 40$, $\sigma_1 = 1$ S/m, $R_1 = 10$ m, $\theta = 10°$, $\phi = 0°$, and f = 3 to 30 MHz

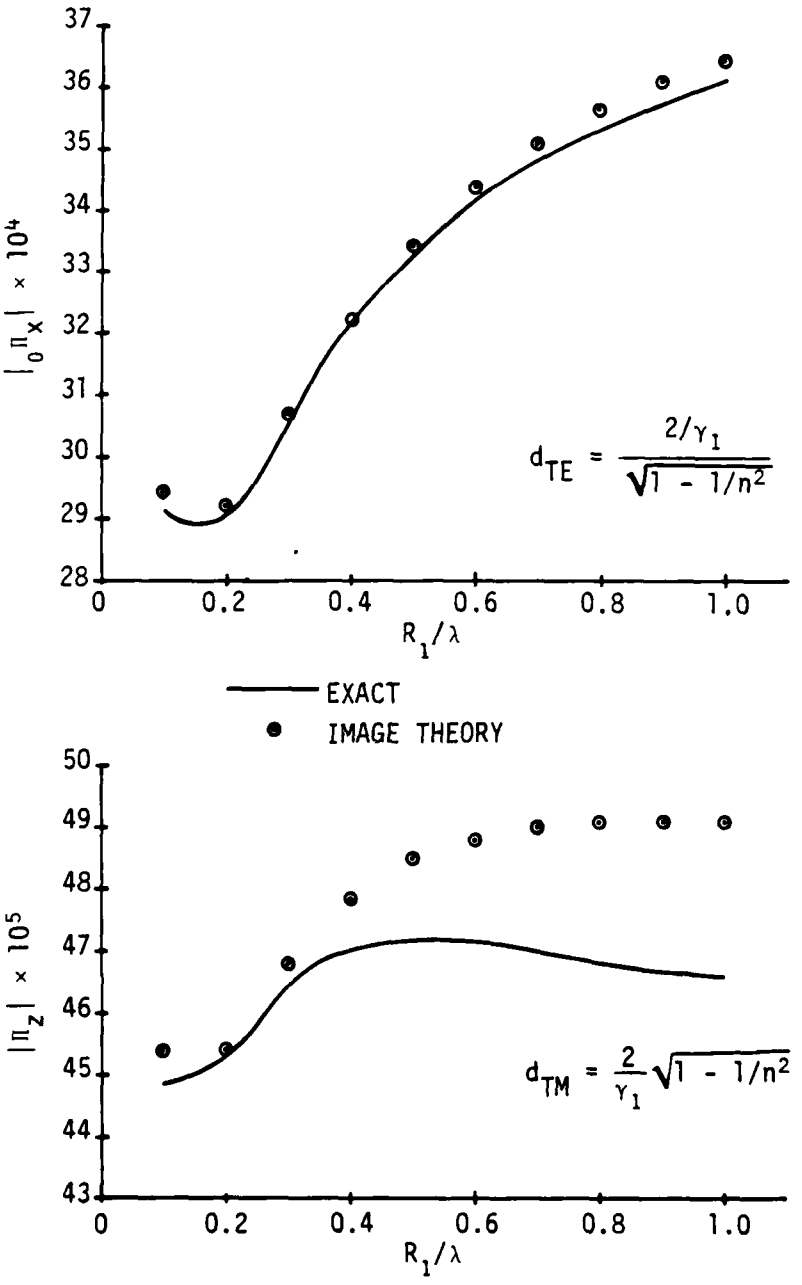

Figure 4. Comparison of Image-Theory and Exact Sommerfeld Integration Results for $\varepsilon_r = 10$, $\sigma_1 = 10^{-2}$ S/m, $R_1 = 10$ m, $\theta = 10°$, $\phi = 0°$, and f = 3 to 30 MHz

EXTENSION TO LARGE NUMERICAL DISTANCES

Image theory also can be utilized to determine the fields at large numerical distances (i.e., $|p| = |-\gamma_0 R_1/2n^2| >> 1$). For the sake of simplicity, we will let $z = h = 0$ and $|n^2| >> 1$. For this case, equation (18) reduces to

$$\Pi_z = \frac{I\ell \cos\phi}{4\pi i\omega\varepsilon_0} \times \frac{\partial}{\partial\rho}\int_0^\infty \left(\frac{2u_0}{u_1 + u_0}\right)\left(\frac{n^2 - 1}{u_1 + n^2u_0}\right)J_0(\lambda\rho)\frac{\lambda}{u_0}d\lambda \ . \tag{45}$$

Since $|\gamma_1\rho| >> 1$, $u_1 \sim \gamma_1 = 2/d$, and

$$\left(\frac{2u_0}{u_1 + u_0}\right) \sim 1 - e^{-u_0 d} \sim u_0 d \ . \tag{46}$$

Furthermore, because $|p| >> 1$,

$$\frac{n^2 - 1}{u_1 + n^2u_0} \sim \frac{n^2 d}{2} e^{-n^2 du_0/2} \ . \tag{47}$$

Therefore,

$$\begin{aligned} \Pi_z &\sim \frac{I\ell d \cos\phi}{4\pi i\omega\varepsilon_0}\left(\frac{n^2 d}{2}\right)\int_0^\infty e^{-n^2 du_0/2} J_0(\lambda\rho)d\lambda \\ &\sim -\frac{I\ell \cos\phi}{2\pi\gamma_1 i\omega\varepsilon_0}\left(\gamma_0^2\right)\left(\frac{n^2 d}{2}\right)^2\left(\frac{\rho e^{-\gamma_0 D}}{D^3}\right) \ , \end{aligned} \tag{48}$$

where $D^2 = \rho^2 + (n^2 d/2)^2$.

Because $\rho^2 >> (n^2 d/2)^2$,

$$\begin{aligned} H_\phi &\sim -i\omega\varepsilon_0\left(\frac{\partial\Pi_z}{\partial\rho}\right) \sim -\frac{I\ell \cos\phi(\gamma_0^2)}{2\pi\gamma_1\rho}\left(\frac{n^2}{\gamma_0\rho}\right)e^{-\gamma_0\rho} \\ &= -\frac{I\ell \cos\phi(\gamma_0^2)e^{-\gamma_0\rho}}{2\pi\gamma_1\rho}\left(-\frac{1}{2p}\right) \ , \end{aligned} \tag{49}$$

which is the correct farfield result for large numerical distances.

CONCLUSIONS

Simple engineering expressions for HED and HMD air-to-air, subsurface-to-air, air-to-subsurface, and subsurface-to-subsurface propagation have been derived by employing finitely conducting earth-image theory techniques. For the air-to-air propagation case, the expressions are valid from the quasi-static to the farfield ranges as long as $|n^2| > 15$ and the Sommerfeld numerical distance is small. For the subsurface-to-air, air-to-subsurface, and subsurface-to-subsurface cases, the additional restriction that the measurement distance be greater than three times the burial depth of the source and/or receiver must be met. We have also demonstrated that image theory can be utilized to determine the fields at large numerical distances.

We have compared successfully image-theory and exact Sommerfeld integration results for four cases, yielding agreement within 1 percent for three comparisons and within 5 percent for the other.

It should be noted that the two media can be inverted and the air replaced by the earth's crust (of conductivity σ_2 and dielectric constant ε_2). The same equations (tables 1 through 8) can be utilized as long as $|\gamma_2 R_1/(2n_2^2)| << 1$ and $|n_2^2| = |\gamma_1^2/\gamma_2^2| > 15$ simply by replacing $i\omega\varepsilon_0$ by $\sigma_2 + i\omega\varepsilon_2$.

The results presented in this report should be particularly useful for sea/air and sea/earth's-crust propagation. They should also be helpful to geophysicists engaged in determining the electrical properties of the earth. The simple, yet accurate, formulas obtained from this theory make it a very strong tool and a promising one for determining the coupling between antennas located above or below the earth's surface.

REFERENCES

1. P. R. Bannister, "Summary of Image Theory Expressions for the Quasi-Static Fields of Antennas At or Above the Earth's Surface," Proceedings IEEE, vol. 67, no. 7, 1979, pp. 1001-1008.

2. P. R. Bannister et al., Quasi-Static Electromagnetic Fields, NUSC Scientific and Engineering Studies, Naval Underwater Systems Center, New London, CT 06320, 1980, 515 pp.

3. J. R. Wait and K. P. Spies, "On the Image Representation of the Quasi-Static Fields of a Line Current Source Above the Ground," Canadian Journal of Physics, vol. 47, no. 23, 1969, pp. 2731-2733.

4. P. R. Bannister, "Extension of Quasi-Static Range Finitely Conducting Earth-Image Theory Techniques to Other Ranges," IEEE Transactions on Antennas and Propagation, vol. AP-26, no. 3, 1978, pp. 507-508.

5. A. Mohsen, "Earth Conductivity Effect on the Field of a Long Horizontal Antenna," IEEE 1980 International Symposium Digest, Antennas and Propagation, vol. 2, 80 CH1557-8AP, 2-6 June, Québec, Canada, 1980, pp. 440-443.

6. S. F. Mahmoud and A. D. Metwally, "New Image Representation for Dipoles Near to a Dissipative Earth, Part I: Discrete Images; Part II: Discrete Plus Continuous Images," Radio Science (in press).

7. E. C. Jordan, Electromagnetic Waves and Radiating Systems, Prentice Hall, Inc., Englewood Cliffs, NJ, 1950, pp. 408-410.

8. A. D. Watt, private communication, 1962.

9. J. R. Wait, "The Electromagnetic Fields of a Horizontal Dipole in the Presence of a Conducting Half-Space," Canadian Journal of Physics, vol. 39, 1961, pp. 1017-1028.

10. A. Sommerfeld, "On the Propagation of Waves in Wireless Telegraphy," Annalen der Physik, vol. 81, no. 25, 1926, pp. 1135-1153.

11. A. Baños, Dipole Radiation in the Presence of a Conducting Half-Space, Pergamon Press, NY, 1966, 245 pp.

12. A. Erdélyi, ed., Tables of Integral Transforms, vol. 2, McGraw-Hill Book Company, Inc., NY, 1954, 451 pp.

13. R. C. Hansen, "Radiation and Reception With Buried and Submerged Antennas," IEEE Transactions on Antennas and Propagation, vol. AP-11, no. 3, 1963, pp. 207-216.

14. K. A. Norton, "The Propagation of Radio Waves Over the Surface of the Earth and in the Upper Atmosphere," Proceedings IRE, vol. 25, no. 9, 1937, pp. 1203-1236.

15. R. J. King, "Electromagnetic Wave Propagation Over a Constant Impedance Plane," Radio Science, vol. 4, no. 3, 1969, pp. 255-268.

16. D. J. Thomson and J. T. Weaver, "The Complex Image Approximation for Induction in a Multilayered Earth," Journal of Geophysical Research, vol. 80, 1975, pp. 123-129.

17. J. R. Wait, Electromagnetic Waves in Stratified Media, Pergamon Press, NY, 1970, pp. 21-31.

18. P. R. Bannister and R. L. Dube, "Simple Expressions for Horizontal Electric Dipole Quasi-Static Range Subsurface-to-Subsurface and Subsurface-to-Air Propagation," Radio Science, vol. 13, no. 3, 1978, pp. 501-507.

19. M. B. Kraichman, Handbook of Electromagnetic Propagation in Conducting Media, U. S. Government Printing Office, Washington, DC, 1970, pp. 3-8 to 3-16.

20. R. Mittra, P. Parhami, and Y. Rahmat-Samii, "Solving the Current Element Problem Over Lossy Half-Space Without Sommerfeld Integrals," IEEE Transactions on Antennas and Propagation, vol. AP-27, no. 6, 1979, pp. 778-782.

INITIAL DISTRIBUTION LIST

Addressee	No. of Copies
DARPA	3
DTIC	15
ONR (Code 425GG (J. Heacock), 428IO (R. G. Joiner))	2
ONR Branch Office, Chicago, (Dr. Forrest L. Dowling)	1
ASN (T. P. Quinn (for C^3), J. Hull (Rm 5E 779)	2
NRL (Library, Dr. J. R. Davis (Code 7550), Dr. Frank Kelly)	3
NOSC (Library, R. A. Pappart, D. G. Morfitt, J. A. Ferguson, F. P. Snyder, C. F. Ramstedt, P. Hansen, K. Grauer, W. Hart)	9
NAVELECSYSCOM (PME 110-11 (Dr. G. Brunhart), PME 110-X1 (Dr. Bodo Kruger), PME 110)	3
NAVAL SURFACE WEAPONS CENTER, WHITE OAK LAB. (J. J. Holmes, M. B. Kraichman, P. Wessel, K. Bishop, R. Brown, J. Cunningham, B. DeSavage, Library)	8
DWTNSRDC ANNA (W. Andahazy, F. E. Baker, P. Field, D. Everstine, B. Hood, D. Nixon)	6
NAVPGSCOL, MONTEREY (O. Heinz, P. Moose, Library)	3
NCSC (K. R. Allen, R. H. Clark, M. J. Wynn, M. Cooper, Library)	5
DIRECTOR, DEFENSE NUCLEAR AGENCY, RAAE, DDST, RAEV	3
R&D Associates, P.O. Box 9695, Marina del Rey, CA 90291 (C. Greifinger , P. Greifinger)	2
Pacific-Sierra Research Corp., 1456 Cloverfield Boulevard, Santa Monica, CA 90404 (E. C. Field)	1
Johns Hopkins University, Applied Physics Laboratory, Laurel, MD 20810 (L. Hart, J. Giannini, H. Ko, I Sugai)	4
University of California, Scripps Institute of Oceanography (C. S. Cox (Code A-030), H. G. Booker, J. Filloux)	4
Lockheed Palo Alto Research Laboratory (W. Imhof, J. B. Reagan, E. E. Gaines, R. C. Gunton, R. E. Meyerott)	5
University of Texas, Geomagnetics and Electrical Geoscience Laboratory (F. X. Bostick, Jr.)	1
COMMANDER, AIR FORCE GEOPHYSICS LABORATORY (J. Aarons)	1
COMMANDER, ROME AIR DEVELOPMENT CENTER (J. P. Turtle, J. E. Rasmussen, W. I. Klemetti, P. A. Kossey, E. F. Altschuler)	5
Applied Science Associates, Inc., (Dr. Gary S. Brown) 105 E. Chatham St., Apex, NC 27502	1
Computer Sciences Corp., Falls Church, VA 22046 (D. Blumberg, Senator R. Mellenberg, R. Heppe, F. L. Eisenbarth)	4
MIT Lincoln Labs. (M. L. Burrows, D. P. White, D. K. Willim, S. L. Bernstein, I. Richer)	5
Electromagnetic Sciences Lab. SRI International, Menlo Park, CA 94025 (Dr. David M. Bubenik)	1
Communications Research Centre (Dr. John S. Belrose) P.O. Box 11490, Station "H" Shirley Bay, Ottawa, Ontario, Canada K2H8S2	1
West Virginia University, Electrical Eng. Dept. (Prof. C. A. Balanis)	1
Dr. Joseph P. deBettencourt, 18 Sterling St., West Newton, MA 02165	1
Dr. Marty Abromavage, IITRE, Div. E., 10W 35th St., Chicago, IL 60616	1
Mr. Larry Ball, U.S. Dept. of Energy NURE Project Office, P.O. Box 2567, Grand Junction, CO 81502	1

INITIAL DISTRIBUTION LIST (Cont'd)

Addressee	No. of Copies
STATE DEPARTMENT ACDA MA-AT, Rm. 5499, Washington, DC 20451 (ADM T. Davies, R. Booth, N. Carrera)	3
GTE Sylvania, (R. Row, D. Boots, D. Esten) 189 B. St. Needham, MA 02194	3
HARVARD UNIVERSITY, Gordon McKay Lab. (Prof. R. W. P. King, Prof. T. T. Wu)	2
University of Rhode Island, Dept. of Electrical Engineering (Prof. C. Polk)	1
Pheonix Corporation (Dr. Robert D. Regan), 1600 Anderson Rd., McLean, VA 22101	1
University of Nebraska, Electrical Engineering Dept., (Prof. E. Bahar)	1
University of Toronto, EE Dept. (Prof. Keith Balmain)	1
NOAA/ERL (Dr. Donald E. Barrick)	1
University of Colorado, EE Dept. (Prof. Petr Beckmann)	1
Geophysical Observatory, Physics & Eng. Lab. DSIR Christchurch, New Zealand (Dr. Richard Barr)	1
U.S. Army Electronic Command Headquarters, Fort Monmouth, NJ (Mr. Morris Acker)	1
General Electric Co., (C. Zierdt, A. Steinmayer) 3198 Chestnut St., Philadelphia, PA 19101	2
University of Arizona, Elec. Eng. Dept., Bldg. 20 (Prof. J. W. Wait) Tuscon, AZ 85721	1
U.S. NAVAL ACADEMY, Dept. of Applied Science (Dr. Frank L. Chi)	1
Stanford University, Radioscience Laboratory (Dr. Anthony Fraser-Smith), Durand Bldg., Rm. 205	1
Stanford University, Stanford Electronics Laboratory (Prof. Bob Helliwell)	1
Colorado School of Mines, Department of Geophysics (Prof. A. Kaufman)	1
Prof. George V. Keller, Chairman, Group Seven, Inc., Irongate II, Executive Plaza, 777 So. Wadsworth Blvd., Lakewood, CO 80226	1
NOAA, Pacific Marine Environ. Lab. (Dr. Jim Larsen)	1
MIT, Dept. of Earth/Planetary Sciences, Bldg. 54-314 (Prof. Gene Simmons)	1
Colorado School of Mines (Dr. C. Stoyer)	1
University of Victoria, (Prof. J. Weaver) Victoria, B.C. V8W 2Y2 Canada	1
Mr. Donald Clark, c/o Naval Security Group Command, 3801 Nebraska Ave., NW, Washington, DC 20390	1
Prof. R. L. Dube, 13 Fairview Rd., Wilbraham, MA 01095	1
U.S. Geological Survey, Rm. 1244 (Dr. Frank C. Frischknecht) Denver, CO 80225	1
Mr. Larry Ginsberg, Mitre Corp., 1820 Dolly Madison Bldg. McLean, VA 22102	1
Dr. Robert Morgan, Rt. 1, Box 187, Cedaredge, CO 81413	1
Mr. A. D. Watt, Rt. 1, Box 183½, Cedaredge, CO 81413	1
Dr. E. L. Maxwell, Atmospheric Sciences Dept., Colorado State University, Fort Collins, CO	1
Mr. Al Morrison, Purvis Systems, 3420 Kenyon St., Suite 130, San Diego, CA 92110	1

INITIAL DISTRIBUTION LIST (Cont'd)

Addressee	No. of Copies
NDRE, Division for Electronics (Dr. Trygve Larsen) P.O. Box 25, Kjeller, Norway	1
Belden Corp., Technical Research Center (Mr. Douglas O'Brien) Geneva, Illinois	1
University of Pennsylvania (Dr. Ralph Showers) Moore School of Elec. Eng., Philadelphia, PA 19174	1
University of Houston, Director, Dept of Elec. Eng. (Prof. Liang C. Shen)	1
The University of Connecticut, Physics Dept., (Prof. O. R. Gilliam), Storrs, CT 06268	1
Dr. David J. Thomson, Defence Research Establishment Pacific, F.M.O., Victoria, B.C., Canada	1
Dr. Robert Hansen, Box 215, Tarzana, CA 91356	1
The University of Kansas, Remote Sensing Laboratory (Prof. R. K. Moore) Center for Research, Inc., Lawrence, Kansas	1
University of Wisconsin, Dept. of Elec. Eng. (Prof. R. J. King)	1
OT/ITS U.S. Dept. of Commerce (Dr. David A. Hill), Boulder, CO	1
Office of Telecommunications, Inst. for Telecommunications Services (Dr. Douglas D. Crombie, Director), Boulder, CO	1
University of Colorado, Dept. of Electrical Eng. (Prof. David C. Chang)	1
Dr. K. P. Spies, ITS/NTIA, U.S. Dept. of Commerce	1
The University of Connecticut, Dept. of Electrical Eng. & Computer Sci., Storrs, CT (Prof. Clarence Schultz, Prof. Mahmond A. Melehy)	2
Dr. Richard G. Geyer, 670 S. Estes St., Lakewood, CO	1
University of California, Lawrence Livermore Lab., (R. J. Lytle, E. K. Miller)	2
Kings College, Radiophysics Group (Prof. D. Llanwyn-Jones) Strand, London WC2R 2LS, England	1
Istituto di Elettrotechnica, Facotta di Ingegneria (Prof. Giorgio Tacconi) Viale Cambiaso 6, 16145 Genova, Italy	1
Universite des Sciences de Lille (Prof. R. Gabillard) B.P. 36-59650 Villeneuve D'Ascq, Lille, France	1
Arthur D. Litte, Inc., (Dr. A. G. Emslie, Dr. R. L. Lagace, R&D Div., Acorn Park, Cambridge, MA 02140	1
University of Colorado, Dept. of Electrical Eng. (Prof. S. W. Maley)	1
University of Washington, EE Dept. (Prof. A. Ishimaru) Seattle	1
Dr. Svante Westerland, Kiruna Geofysiska Institute S981 01 Kiruna 1, Sweden	1
Dr. Harry C. Koons, The aerospace Corp., P.O. Box 92957, Los Angeles, CA 90009	1
Dr. Albert Essmann, Hoogewinkel 46, 23 Kiel 1, West Germany	1
Glenn S. Smith, School of Elec. Eng. Georgia Tech. Atlanta, GA	1
Dr. T. Lee, CIRES, Campus Box 449, University of Colorado	1
Dr. Jack Williams, RCA Camden, Mail Stop 1-2, Camden, NJ 08102	1
Dr. Joseph Czika, Science Applications, Inc., 840 Westpark Dr. McLean, VA 22101	1
Mr. Arnie Farstad, 390 So. 69th St., Boulder, CO 80303	1

INITIAL DISTRIBUTION LIST (Cont'd)

Addressee	No. of Copies
NATO SACLANT ASW CENTER (Library)	1
USGS, Branch of Electromagnetism and Geomagnetism (Dr. James Towle) Denver, CO	1
NOAA, Pacific Maine Environ. Lab. (Dr. Jim Larsen)	1
University of Texas at Dallas, Geosciences Division, (Dr. Mark Landisman)	1
University of Wisconsin, Lewis G. Weeks Hall, Dept. of Geology and Geophysics (Dr. C. S. Clay)	1
DCA/CCTC, Def Communication Agency, Code C672 (Dr. Frank Moore)	1
Argonne National Laboratory, Bldg. 12 (Dr. Tony Vallentino)	1
IITRE, Div. E, Chicago (Dr. Marty Abromavage)	1
The University of Manitoba, Elec. Eng. Dept. (Prof. A. Mohsen)	1
Mr. Jerry Pucillo, Analytical Systems, Engineering Corp., Newport, RI 02840	1
Dr. Misac N. Nabighian, Newmont Exploration Ltd., Tuscon	1
Dr. Fred Raab, Pohemus, P.O. Box 298, Essex Junction, VT 05452	1
Dr. Louis H. Rorden, President, Develco, Inc., 404 Tasman Dr. Sunnyvale, CA 94086	1
Dr. D. D. Snyder, EDCON, 345 South Untion Blvd, Lakewood, CO	1
Dr. Eivind Trane, NDRE, P.O. Box 25, 2007 Kjeller, Norway	1
RCA David Sarnoff Research Center (K. Powers, J. Zennel, L. Stetz, H. Staras)	4
University of Illinois, Aeronomy Laboratory (Prof. C. F. Sechrist)	1
Dr. Cullen M. Crain, Rand Corp., Santa Monica	1
Radioastronomisches Institute der Universität Bonn (Dr. H. Volland), 5300 Bonn-Endenich, Auf dem Hiigel 71 West Germany	1
Dr. John P. Wikswo, Jr., P.O. Box 120062 Acklen Station, Nashville	1
Mr. Lars Brock-Nannestad, DDRB Osterbrogades Kaserne, 2100 Copenhagen O, Denmark	1
Institut de Physique du Globe (Dr. Edonard Selzer) 11 Quai St., Bernard, Tour 24 Paris Ve, France	1
Elektrophysikalisches Institut (Dr. Herbert König) Technische Hochschule, Arcisstrasse 21, 8 Munich 2, West Germany	1
Raytheon Company (Dr. Mario Grossi) Portsmouth, RI	1
NISC, Code 00W (Mr. M. A. Koontz) Washington, DC	1
Polytechnic Institute of Brooklyn (Prof. Leo Felsen)	1
NOAA/ERL (Dr. Earl E. Gossard) R45X7, Boulder, CO 80302	1
Dr. George H. Hagn, SRI-Washington, Rosslyn Plaza, Arlington	1
NOAA/ERL (Dr. C. Gordon Little) R45	1
Goddard Space Flight Ctr. (Dr. S. H. Durrani) Code 950	1
ITS, Office of Telecom (Dr. Ken Steele) Boulder, CO 80302	1
NTIA/ITS, U.S. Dept. of Commerce (Dr. A. D. Spaulding)	1
Stanford University, Elec. Eng. Dept. (Dr. O. G. Villard, Jr.)	1
Dr. D. Middleton, 127 East 91st St., New York, NY 10028	1
University of California, Elec. Eng. & Computer Sci. Dept., (Prof. K. K. Mei)	1

INITIAL DISTRIBUTION LIST (Cont'd)

Addressee	No. of Copies
California Inst. of Technology, Jet Propulsion Lab., (Dr. Yahya Rahmat-Samii)	1
Raytheon Service Co. (Dr. M. Soyka) Mt. Laurel, NJ 08054	1
MITRE M/S W761 (Dr. W. Foster) McLean, VA	1
Max-Planck-Institut fur Aeromomie (Prof. P. Stubbe) 3411 Katlenburg-Lindau 3 FRG	1
University of Otago, Physics Dept. (Prof. R. L. Dowden) Dunedin, New Zealand	1
University of Leicester, Physics Dept. (Prof. T. B. Jones) Leicester, England	1
Naval Weapons Center, China Lake, Code 3814 (Dr. R. J. Dinger)	1
Dr. Claudia D. Tesche, Lutech, Inc., P.O. Box 1263, Berkeley	1
National Aeronautical Est., National Research Council, Flight Research Lab., (Dr. C. D. Harwick) Ottawa, K1AOR6, Canada	1
Colorado Research and Prediction Laboratory, Inc. (Dr. R. H. Doherty, Dr. J. R. Johler) Boulder, CO	2